NUMERICAL MODELLING OF AC ELECTRIC ARCS

H. L. Larsen, A. Hildal, V.G. Sevastyanenko* and J. A. Bakken

Dept. of Metallurgy, Norwegian Institute of Technology, N-7034 Trondheim, NORWAY
*Dept. of Technical Physics, Belorussian Polytechnic Academy, Minsk, BELARUS

ABSTRACT. A 2D-numerical model for alternating current (AC) electric arcs is developed. The time dependent equations for mass, momentum and energy are solved together with the conservation equation for the magnetic field. The momentaneous current is calculated by solving the single-phase circuit equation of the arc furnace. Two methods for calculating the radiation from the arc is tested, the integral method of partial characteristics and the conventional method assuming an effective arc radiation radius. Solution of the coupled set of differential equations gives the total arc voltage and current, the current density distribution, the temperature, pressure and velocity fields as functions of time.

INTRODUCTION

Numerical modelling of electric arcs by solving the magnetohydrodynamic equations has until recently been restricted to steady-state arcs (DC). However, having more powerful computers available, the possibility of modelling also time-dependent phenomena as *alternating current* (AC) arcs is offered. AC arcs are used in many industrial processes, e.g. in arc welding and in three-phase electric arc furnaces for steel-making and submerged-arc furnaces for production of silicon metal and ferrosilicon. The current levels range from some hundred amperes in welding arcs to above 100 kA in arc furnaces. The AC model presented here is therefore tested on both a *low* current arc in argon (I_{rms}~ 1000 A), and a *high* current arc in the crater of a 30 MVA silicon metal furnace where the crater gas consists of Si-O-C compounds (I_{rms}~ 100 kA).

DESCRIPTION OF THE MODEL

Assumptions and equations

The model will only be briefly described here, as the details are found in a previous paper /1/. The arc is assumed to be *cylindrically symmetric* and in *local thermodynamic equiliblium* (LTE). The *time dependent* conservation equations for mass, momentum and energy are solved. The source terms S_ϕ in the energy equation consists of ohmic heating in the arc, energy transported by electrons and radiation loss. The components of the Lorentz-force $\boldsymbol{F} = \boldsymbol{j} \times \boldsymbol{B}$ are source terms in the momentum equations and give rise to a gas jet towards the anode. In addition a conservation equation for the magnetic field is deduced from Ohm's law and Maxwell's equations.

The model is implemented in a modified version of the commercial fluid flow and heat transfer programme FLUENT and calculations are carried out on a HP9000/755 computer. Time steps of 0.01-0.02 ms are used in the calculations.

The electric circuit

The arc is a non-linear circuit element in an electric circuit consisting of an ideal voltage source with rms value U_{rms}, a loss resistance r and an inductance L. The voltage drop across the plasma LTE region is calculated, and the cathode and anode fall voltages, U_{an} and U_{ca}, are estimated. The calculated voltage drop over the plasma column, u_{arc}, also includes the induced voltage due to the magnetic flux through the modelling domain. The anode and cathode falls are modelled with a step-function, i.e. the sign of the fall voltages change when the current changes direction. The current is not given a priori, but is calculated by a first order time integration of *the circuit equation*:

$$\sqrt{2}\,U_{rms}\cos(\omega t) = L\frac{di}{dt} + ri + u_{\text{arc}} + U_{an} + U_{ca}\,, \quad \omega = 2\pi f\,, \quad f = 50Hz \qquad (1)$$

Thermophysical properties and radiation data

The thermophysical properties (density, entalphy, viscosity, thermal and electric conductivity) for *argon* and *Si-O-C* gas mixtures were calculated by Gu /2/. Volumetric radiation densities for argon were also calculated by Gu /3/, absorption was taken into account by considering the radiation escaping from an isothermal sphere of radius R_{eff}. Another method for calculating the radiation density, Sevastyanenko's *integral method of partial characteristics* (IMPC) /4/ was also tested for argon as well as Si-O-C. The radiation density is expressed as

$$S_{rad} = \int_{4\pi} \nabla\cdot\vec{I}\; d\omega = \int_{4\pi}\left(\int_0^{\infty} I_\nu^0(x)\,k_\nu'(x)\,d\nu - \int_0^{\infty} k_\nu'(x)\int_0^{x} I_\nu^0(\xi)\,k_\nu'(\xi)\exp\left[-\int_\xi^{x} k_\nu'(\eta)\,d\eta\right]d\xi\,d\nu\right)d\omega \qquad (2)$$

where k_ν' is the spectral absorption coefficient and I_ν^0 is the Planck function. $\nabla\cdot\vec{I}$ is the difference between radiation emmited from the point under consideration x, and radiation absorbed at x originating from sources ξ, lying on the ray between the boundary of the radiating volume and x. A *linear temperature distribution* is assumed between x and the boundary and between x and the partial sources ξ. The integration over frequencies was calculated a priori. The integration over space is carried out during the arc calculation.

RESULTS AND DISCUSSION

A. Low current laboratory arcs (~1000 A) in argon

In order to test the AC model by relatively low currents (~ 1000 A) measurements of current and voltage of an argon arc burning between graphite electrodes have been carried out in a water-cooled chamber /5/. Two series-connected welding transformers with an adjustable built-in inductance were used as a voltage source in the experiments. By replacing the arc with known resistances, the inductance and resistance of the external circuit were measured for different settings of the transformer inductance, which constitutes the main part of the external impedance. A schetch of the arc chamber with the modelling domain is shown in Fig.1. Two cases with different electric circuit parameters were simulated and compared with measurements, see Table 1 and Fig.2.

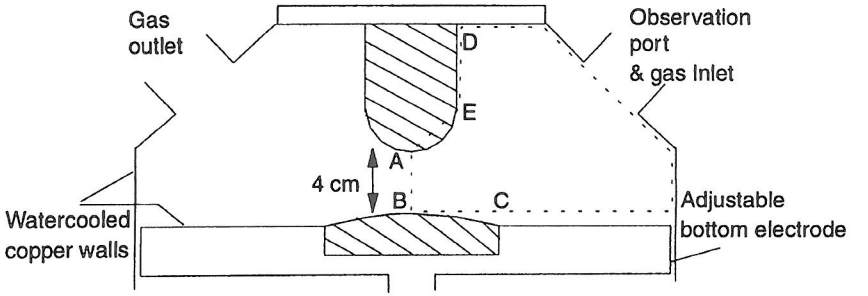

Fig.1. Schetch of the arc chamber and the corresponding modelling domain (ABCDE)

Table 1. Measured (averaged over some minutes with standard deviation) and calculated rms current and voltage for low current laboratory arcs

Arc length=4 cm,	$j_c = 4.4 \cdot 10^7$ A/m^2	I_{rms} (A)	U_{rms} (V)
(a) U_{rms} = 192V	Measured	651 ± 8	44 ± 1
r = 0.03 Ω	Calc., R_{eff} = 1 cm	695	35
L = 0.84 mH	Calc., IMPC	694	40
(b) U_{rms} = 195V	Measured	946 ± 8	48 ±2
r = 0.02 Ω	Calc., R_{eff} = 1 cm	1032	39
L = 0.57 mH			

A parabolic distribution of the current density on the cathode is assumed. The *mean* value used, $j_c = 4.4 \cdot 10^7$ A/m^2, is based on observations of the cathode spot of AC arcs with currents 4-8 kA /6/. The temperature on the cathode is 4413 K and on the sourrounding walls 273 K. The no-slip condition for velocity is used on all walls and normal symmetry conditions on the axis AB. The magnetic field on the cathode surface is calculated from the given current distribution and the magnetic field on the anode is perpendicular to the surface. The magnetic field on the walls is a function of radius and total current /1/. The fall voltages were set at $U_{an} = U_{ca} = 5V$.

Fig. 2 shows that the waveforms of measured and calculated voltage and current are in good agreement. Fourier analysis show that both the measured and the calculated current waveforms contain a DC component. The measured value was 84 A while the calculated were only 22 A (R_{eff}) and 51 A (IMPC). Fourier analysis of the measured and calculated voltages shows that the relative sizes of the different harmonics are in good agreement. The measured DC component of the voltage is negligible (-0.16 V) and within the measurement uncertainty, whereas the calculated DC components are -0.48 V (R_{eff}) and -0.46 V (IMPC).

When comparing the measurements and calculations some visual observations must be kept in mind. By using a high speed camera the arc was observed to be less "bell

shaped" with a more diffuse cathode spot in the half period when the upper electrode was anode. This may explain the higher DC component in the measured current. The arc was also seen to burn unsteadily and preferred to attach to the egde of the bottom electrode. This probably gave an increased "effective" arc lenght and thereby a higher voltage than the ideal stable arc modelled. A comparison between measured and calculated waveforms for case b) gave similar results.

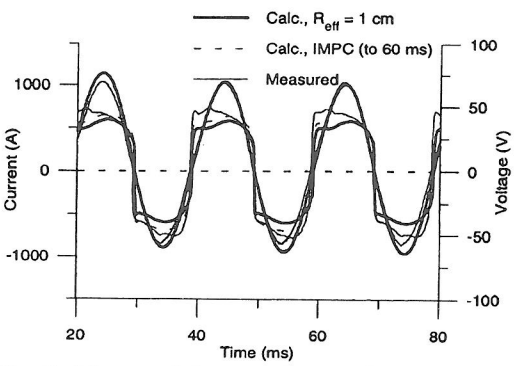

Fig. 2. Measured (averaged over sixteen 50 Hz periods) and calculated voltage and current vs. time for case a)

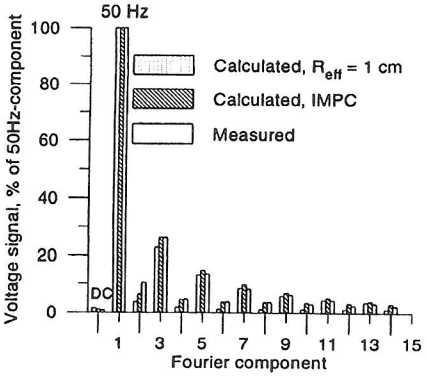

Fig. 3. Fourier components of the measured and calculated voltage

The most uncertain parameter in the calculations is the cathode current density. We know that an increase of the mean current density will increase the arc resistance and thereby increase the voltage and decrease the current. An increase of the cathode and anode fall would shift the modelling results in the same direction.

Using the IMPC-method for the arc radiation gave a slightly increased arc voltage, but did not change the current/voltage characteristics dramatically as seen in Fig. 2. The main advantage of this method is that the choice of an "effective" radiation radius is avoided. Especially in AC arcs where the arc expands and contracts as the current varies, the assumption of an effective arc radius might be doubtful. However, using the IMPC method increased the computing time by a factor of three. The results obtained in the high temperature arc core (T > 8000 K) were quite reasonable, but the radiation absorbed in the low temperature zone seemed to be overestimated because of the assumption of linear temperature profiles. The accuracy could be increased by using higher order approxiametions to the temperature profile between x and the boundary and between x and the sources ξ.

The use of the k-ε turbulence model with standard coefficients on case a) gave a more "expanded" arc, e.g. the isotherms were more smeared out /1/. The effect on the calculated current was neglible and the rms voltage was decreased by about 2%.

B. High current industrial arcs (~100 kA) in Si-O-C

The AC arc model was also tested on an industrial arc in a silicon-metal furnace, where the crater gas consists of Si-O-C compounds. The Si/O/C ratio of the gas mixture is given by the SiO/CO-ratio required for liquid silicon to form with a realistic recovery in the crater. In the calculations presented here a SiO/CO-ratio of 2 is used. The arc radiation was calculated according to the IMPC-method. A schetch of the furnace crater with the corresponding modelling domain is presented in Fig. 4. Similar boundary conditions as described in the last section are used, despite of the crater wall temperature which is 2000 K. However, the mean cathode current density was decreased to $j_c = 1.0 \cdot 10^7 A/m^2$. The arc lenght used was 5 cm.

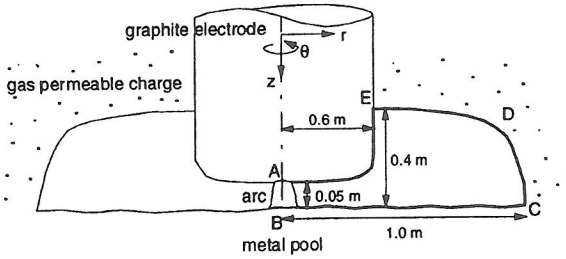

Fig. 4. Schetch of the silicon metal furnace and the modelling domain (ABCDE)

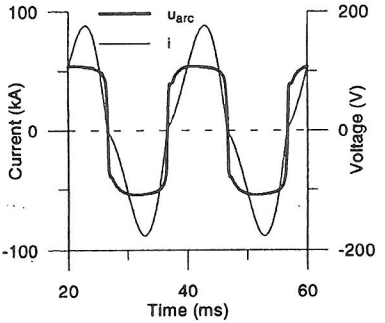

Fig. 5. Calculated voltage and current vs. time for the arc in a silicon metal furnace

Elkem has provided typical parameters (per phase) for the electrical circuit of a 22 MW three-phase silicon metal furnace: $U_{sec} = 133\ V$, $L = 3.82\ \mu H$, $r = 0.1\ m\Omega$. The cathode and anode falls were set at $U_{ca} = U_{an} = 5\ V$. The power per phase is ~7.3 MW, which gives an arc power of ~6.7 MW. The measured rms arc current and voltage is ~77 kA and ~88 V. Our calculations, which are presented in Fig. 5, give an rms current of 59 kA and an arc voltage of 100 V. The calculated power is 5.4 MW.

By comparing our modelling results with the measured values the calculated arc resistance is higher than in the real industrial furnace. This gives higher rms voltage and lower current than the measured ones. Important parameters which must be chosen in the calculations are the *arc lenght*, *the cathode current density* and *the anode and cathode falls*. Increased values of these parameters will all increase the arc resistance further.

However, the real arc power may also be lower than 6.7 MW. Some of the current - e.g. 10% - will probably pass through the charge. To adjust for this a resistance in parallel with the arc could be included in the circuit equation. Impurities, e.g. calsium and aluminium may also contribute to reducing the resistance in the real arc, but our

transport coefficients, thermodynamic data and radiation properties do not take any such effects into account.

Preliminary calculations on the high current arc using thermophysical data for 1 bar indicated that the pressure gradients due to constriction of the arc at the cathode and stagnation flow at the anode were significant. The pressure in these areas was about 1 bar higher than on the crater walls at maximum current. Pressure dependent thermophysical properties were therefore included in the model and the energy conservation equation was modified with the term *Dp/Dt*. The radiation properties, which are also pressure dependent, were , however, not modified. These modifications had a surprisingly negligible effect on the calculated current and voltage.

CONCLUSION

The AC arc model gives satisfactory agreement between measured and calculated current and voltage for relatively low current arcs (~1000 A) in argon. The IMPC-method for calculating radiation from the arc is suitable in the high temperature core of the arc , but overestimates absorption in the low temperature surroundings. It is more difficult to obtain good agreement for the high current arcs (~100 kA), the modelling results for arcs in SiO/CO give a higher arc resistance than measured in an industrial furnace.

ACKNOWLEDGEMENTS

This work has been supported by The Reasearch Association of the Norwegian Ferroalloys Industry (FFF) and The Royal Norwegian Research Council (NFR). Gu Liping is thanked for implementing the IMPC-method in the FLUENT code and Roar Jensen for valuable assistance during the experimental work.

REFERENCES

/1/ Larsen, H. L., Bakken, J. A.; *A time dependent numerical model for an AC electric arc*, 3rd European Congress on Thermal Plasma Processes, 19.- 21. Sept. 1994, Aachen, Germany

/2/ Gu, L.; *Thermodynamic and transport properties of and diffusion in (Ar-) Si-O-C plasma mixtures*, SINTEF Materials Technology report, STF24 A94546, 1994

/3/ Gu, L.; *Transport phenomena in silicon vapour infiltrated argon arcs and anodic metal pools*, Ph.D. thesis, Dept. of Metallurgy, Norwegian Institute of Technology, 1993

/4/ Sevastyanenko, V. G., Gu, L., Bakken, J. A.; *Radiative Gas-Dynamics in multicomponent plasma*, International Symphosium on Heat and Mass Transfer under Plasma Conditions, 4.- 8. July 1994, Cesme, Turkey

/5/ Hildal, A.; *Measurements of AC arc characteristics*, M.Sc. thesis, Dept. of Metallurgy, Norwegian Institute of Technology, 1994 (in Norwegian)

/6/ Jordan, G. R., Bowman, B., Wakelam, D.; *Electrical and photographic measurements of high-power arcs*, J. Phys. D: Appl. Phys., Vol. 3, 1970